electronics

Article

Simple Learning-Based Robust Trajectory Tracking Control of a 2-DOF Helicopter System

Mahmut Reyhanoglu [1,*], Mohammad Jafari [1] and Muhammad Rehan [2]

[1] Robotics Engineering Program, Columbus State University, Columbus, GA 31907, USA; jafari_mohammad@columbusstate.edu
[2] ESG Automotives, Troy, MI 48083, USA; muhammad.rehan@esg-usa.com
* Correspondence: reyhanoglu_mahmut@columbusstate.edu;

Abstract: Stabilization and tracking control of Unmanned Aircraft Systems (UASs) such as helicopters in a complex environment with system uncertainties, unknown disturbances, and noise is a challenging task; therefore, to compensate for system uncertainties and unknown disturbances, this paper presents a trajectory tracking control strategy for a 2-DOF (degree of freedom) helicopter system testbed by employing a gradient descent-based simple learning control law that minimizes the cost function corresponding to desired closed-loop error dynamics of the nonlinear system under control. In addition, to ensure the stability of the closed-loop nonlinear system, further analysis is provided. The learning capability of the designed controller makes it suitable to take system uncertainties and unknown disturbances into account. The results of computer simulations and real-time experiment using the Quanser AERO helicopter are included to demonstrate the effectiveness of the designed control strategy.

Keywords: learning control; trajectory tracking; nonlinear control; helicopter

Citation: Reyhanoglu, M.; Jafari, M.; Rehan, M. Simple Learning-Based Robust Trajectory Tracking Control of a 2-DOF Helicopter System. *Electronics* **2022**, *11*, 2075. https://doi.org/10.3390/electronics11132075

Academic Editors: Moad Kissai, Bruno Monsuez and Barys Shyrokau

Received: 7 June 2022
Accepted: 29 June 2022
Published: 1 July 2022

1. Introduction

Unmanned Aircraft Systems (UASs) are being employed in a wide range of applications including reconnaissance and mapping, search and rescue, environmental monitoring, and power-line, wind turbine, and bridge inspection to name a few [1,2]. In general, they are categorized into fixed-wing crafts, airship/dirigible balloons, and rotary craft classes [1,2]. These systems are inherently unstable and designing controllers for them requires rigorous consideration and therefore they attracted significant attention in the recent past. Several examples have been studied in the context of fixed-wing crafts [3,4] and rotary-craft UASs such as helicopters [5–19], tricopters [20], quadcopters [21–26], and hexacopters [27].

A helicopter is one of the most flexible types of rotary-craft UASs with horizontally spinning rotors that supply the thrust and lift. This structure provides the capabilities of Vertical Takeoff and Landing (VTOL), hovering, and flying in different directions. Numerous linear and nonlinear control strategies have been designed to control helicopters. Linear control techniques for helicopters include Proportional-Integral-Derivative (PID), Linear-Quadratic-Regulator (LQR), and linearization-based adaptive and optimal control methods [5–8]. For example, based on linear quadratic techniques, an adaptive augmentation method was designed and experimentally applied to control the Quanser 2-DOF helicopter in [5]. The authors in [6] developed an optimal LQR controller for the attitude tracking control of the 2-DOF helicopter. In their work, the authors utilized the Adaptive Particle Swarm Optimization (APSO) approach to acquire the Q and R matrices. In another study [7], a control framework has been designed to track desired trajectories for the 2-DOF helicopter by applying an extended linearization method. Later, the authors in [8] developed a Multi-Step Q-Learning (MsQL) method for solving the optimal output regulation

problem for the Quanser 2-DOF helicopter. Although these linear control techniques are relatively easy to design and implement, their operational range is limited.

As helicopter systems are inherently nonlinear and due to numerous sources of uncertainties and disturbances, there remain many open problems in the design of control algorithms that can effectively compensate for these challenges; therefore, simple linear control strategies may not be effective in meeting the desired performance requirements [27]. To this end, in this paper, we focus on developing robust nonlinear control strategies for tracking control of the 2-DOF helicopter systems. In the past few years, several studies have been devoted to designing and validating nonlinear adaptive and robust controllers to better compensate for the nonlinearity, uncertainties, and disturbances in the 2-DOF helicopter systems. For example, a backstepping controller has been designed by incorporating nested saturation feedback functions for tracking control of helicopters in [14]. In a relevant study [28], to independently track the yaw and pitch position references, a backstepping adaptive nonlinear controller has been designed. The authors in [16] implemented an optimized fractional-order sliding mode controller (SMC) on the 2-DOF Quanser AERO helicopter testbed where they chose the sliding surface in a fractional-order hyperplane in order to reduce the chattering. Other nonlinear and learning-based control strategies developed for helicopter systems can be found in [11–13,15,17–19].

In our previous work [9], to achieve both asymptotic regulation to desired set points and trajectory tracking of a 2-DOF helicopter system an observer-based SMC strategy is developed. Moreover, to prove set point stabilization and robust trajectory tracking of the helicopter, and the convergence of the velocity estimates, Lyapunov-based analyses are provided. In [10], to achieve robust nonlinear tracking control of the 2-DOF helicopter system, we extended our results in [9] by replacing the sliding mode observer with a bank of dynamic filters. Furthermore, to illustrate the effectiveness of the dynamic filter-based tracking control strategy, numerical simulation and experimental results are provided using the Quanser 2-DOF AERO helicopter.

Although all these nonlinear and learning-based methods have several advantages such as dealing with uncertainties and disturbances, they are mostly computationally expensive to be implemented in real-time. To this end, in this paper, we follow the key steps presented in [20] for the design of a simple learning control strategy for the trajectory tracking of a 2-DOF helicopter system. Our main contributions in this paper are as follows:

i Development of a simple learning based robust control algorithm that is computationally efficient for real-time implementation.
ii Demonstration of the effectiveness of the proposed tracking control law via experimental results using the Quanser 2-DOF AERO helicopter.

The rest of this paper is organized as follows: the mathematical model of the 2-DOF helicopter system is presented in Section 2. In Section 3, the gradient descent-based simple learning control strategy design is investigated and discussed. We illustrate the satisfactory performance of the proposed method by providing several numerical simulations and experimental implementation in Section 4, and finally conclusions and further extensions are presented in Section 5.

2. Mathematical Model

Consider the schematic representation of a 2-DOF helicopter system shown in Figure 1, where the right-handed frame B is a body-fixed frame with axes x, y, and z. The system has two identical propellers. The horizontal propeller generates a thrust force F_p at distance r_p, which results in a pitch torque around the y-axis. The vertical propeller generates a thrust force F_y at distance r_y, which results in a yaw torque abut the z-axis.

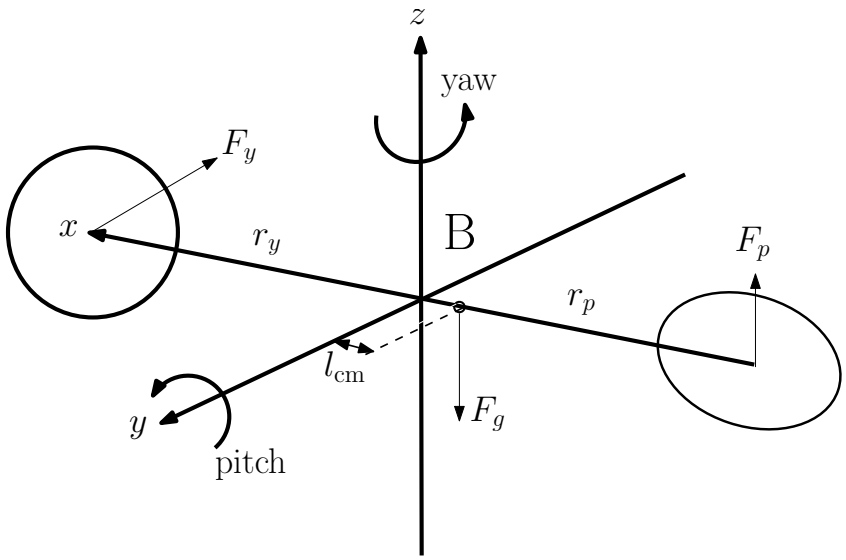

Figure 1. Schematic representation of the Quanser 2-DOF AERO helicopter.

Let θ and ψ denote the pitch and yaw angles, respectively. Then, the dynamical model of the helicopter can be expressed as [9]:

$$\ddot{\theta} = \frac{1}{a_1}[K_{pp}V_p + K_{py}V_y + a_2] \tag{1}$$

$$\ddot{\psi} = \frac{1}{b_1}[K_{yp}V_p + K_{yy}V_y + b_2] \tag{2}$$

where

$$a_1 = J_p + ml_{cm}^2$$
$$a_2 = -mgl_{cm}\cos\theta - D_p\dot{\theta} - ml_{cm}\dot{\psi}^2\sin\theta\cos\theta$$
$$b_1 = J_y + ml_{cm}^2\cos^2\theta$$
$$b_2 = -D_y\dot{\psi} + 2ml_{cm}^2\dot{\psi}\dot{\theta}\sin\theta\cos\theta$$

where m is the helicopter mass, l_{cm} is the distance between the center of mass and the point of rotation, (D_p, D_y) are viscous friction coefficients, $(K_{pp}, K_{py}, K_{yp}, K_{yy})$ are the thrust torque constants, and J_p and J_y are moments of inertia (MOIs) around the pitch and yaw axes, respectively. The control input voltages to the DC torque motors are V_p and V_y, which control the pitch and yaw propellers, respectively. These input voltages are restricted to $[-24, 24]$ V.

3. Control Design

Consider the nonlinear dynamical system defined by (1) and (2). Define the following input transformation from (V_p, V_y) to (u_1, u_2):

$$\begin{bmatrix} u_1 \\ u_2 \end{bmatrix} = \begin{bmatrix} K_{pp} & K_{py} \\ K_{yp} & K_{yy} \end{bmatrix} \begin{bmatrix} V_p \\ V_y \end{bmatrix} \tag{3}$$

so that (1) and (2) can be rewritten as

$$\ddot{\theta} = \frac{1}{a_1}(u_1 + a_2) \tag{4}$$

$$\ddot{\psi} = \frac{1}{b_1}(u_2 + b_2) \tag{5}$$

Clearly, each of these two equations can be written in the following form:

$$\dot{x}_1 = x_2 \tag{6}$$
$$\dot{x}_2 = f(x) + g(x)u + d \tag{7}$$

where the state vector and control input are defined as $x = [x_1, x_2]^T \in \mathbb{R}^2$ and $u \in \mathbb{R}$, respectively. The modeling uncertainties and external disturbances are lumped together as disturbance $d \in \mathbb{R}$, which is assumed bounded. The control objective is to design a control input u such that the system tracks the given reference trajectory $r(t) = [r_1(t), r_2(t)]^T$, where $r_2 = \dot{r}_1$, while all the states and input remain bounded.

Remark 1. *Although there exist several works on UASs or similar systems such as [29,30], which do not require any knowledge of system parameters, our work demonstrates that considering some information about the dynamics of the system could significantly reduce the computational complexity of the designed controller and make it suitable for real-time implementation; however, one can extend our results by designing an approximator to estimate the system parameters, e.g., [21].*

Define the tracking error variables

$$e_1 = r_1 - x_1 \tag{8}$$
$$e_2 = r_2 - x_2 \tag{9}$$

and consider the following control input:

$$u = g^{-1}(x)\left[-f(x) + k_1 e_1 + k_2 e_2 + \dot{r}_2 - \hat{d}\right] \tag{10}$$

where $\hat{d}$ is the estimated disturbance and $k_i > 0,\ i = 1, 2$, are control gains. Then the closed-loop error dynamics can be derived as follows

$$\dot{e}_1 = e_2 \tag{11}$$
$$\dot{e}_2 = -k_2 e_2 - k_1 e_1 - d + \hat{d} \tag{12}$$

For robust control performance, the desired closed-loop error dynamics defined as

$$c(e, k^{\text{des}}) = \dot{e}_2 + k_2^{\text{des}} e_2 + k_1^{\text{des}} e_1 \tag{13}$$

should converge to zero. Here gradient decent method is used for the minimization of the closed-loop error function (or the cost function) given by

$$C = \frac{1}{2}(c(e, k^{\text{des}})^2 \tag{14}$$

The time-update rule for controller gains is given by

$$\dot{k}_i = -\alpha \frac{\partial C}{\partial k_i} = \alpha_i c(e, k^{\text{des}}) e_i \tag{15}$$

where $\alpha_i > 0$ is the learning rate for the i^{th} controller gain. Similarly, the update rule for the disturbance estimate is

$$\dot{\hat{d}} = -\alpha_{\hat{d}} \frac{\partial C}{\partial \hat{d}} = -\alpha_{\hat{d}} c(e, k^{\text{des}}) \tag{16}$$

where $\alpha_{\hat{d}}$ is the learning rate for the disturbance estimate $\hat{d}$. The controller gains and disturbance estimates are updated until the cost function goes to zero, i.e., $C(e, k^{\text{des}}) = 0$.

Stability Proof

The closed-loop error dynamics can be rewritten as

$$\ddot{e}_1 + k_2\dot{e}_1 + k_1 e_1 - \hat{d} + d = 0 \tag{17}$$

We assume that the average rate of change of the disturbance d is much smaller than that of the error state variables so that taking the time derivative of (17) with $\dot{d} = 0$ yields

$$\dddot{e}_1 + k_2\ddot{e}_1 + (k_1 + \dot{k}_2)\dot{e}_1 + \dot{k}_1 e_1 - \dot{\hat{d}} = 0 \tag{18}$$

Plugging the expressions for $\dot{k}_i$ and $\dot{\hat{d}}$ in (18) yields

$$\dddot{e}_1 + a_1(\xi)\ddot{e}_1 + a_2(\xi)\dot{e}_1 + a_3(\xi)e_1 = 0 \tag{19}$$

where $\xi = [e_1\ \dot{e}_1\ \ddot{e}_1]^T$ is the state and

$$a_1(\xi) = k_2 + \alpha_{\hat{d}} + \beta(\xi),\ a_2(\xi) = k_1 + k_2^{\text{des}}(\alpha_{\hat{d}} + \beta(\xi)) \tag{20}$$

$$a_3(\xi) = k_1^{\text{des}}(\alpha_{\hat{d}} + \beta(\xi)),\ \beta(\xi) = \alpha_1 e_1^2 + \alpha_2 \dot{e}_1^2 \tag{21}$$

Equation (19) is in a pseudo-linear form. Following [31], we perform a Routh–Hurwitz criterion-based stability analysis. Clearly, $a_i(\xi) > 0,\ i = 1, 2, 3, \forall \xi$ and the characteristic equation corresponding to $a_i(0),\ i = 1, 2, 3$, is given by

$$s^3 + a_1(0)s^2 + a_2(0)s + a_3(0) = 0 \tag{22}$$

Applying the Routh–Hurwitz criterion, it can be shown that all the roots of characteristic Equation (22) have negative real parts if $a_1(0)a_2(0) > a_3(0)$, where

$$a_1(0) = k_2 + \alpha_{\hat{d}},\ a_2(0) = k_1 + k_2^{\text{des}}\alpha_{\hat{d}},\ a_3(0) = k_1^{\text{des}}\alpha_{\hat{d}} \tag{23}$$

Equivalently, the closed-loop error system is asymptotically stable if

$$k_2^{\text{des}}\alpha_{\hat{d}}^2 + (k_1 + k_2 k_2^{\text{des}} - k_1^{\text{des}})\alpha_{\hat{d}} + k_1 k_2 > 0 \tag{24}$$

In what follows, we choose $k_i,\ k_i^{\text{des}}$, and $\alpha_{\hat{d}}$ such that this stability condition is satisfied.

4. Numerical Simulation and Experimental Results

This section presents the results of computer simulations and experimental implementation of the 2-DOF helicopter control under three different scenarios. The performance of the control law proposed in Section 3 is evaluated using the system parameters of the Quanser AERO 2-DOF helicopter. Nominal and estimated system parameters are given in Tables 1 and 2, respectively. It is worth noting that the proposed controller is robust to variation in system parameters meaning that regardless of using the values in Table 1 or Table 2, the performance of the developed controller is satisfactory. The performance of the proposed method is further validated by comparing it to PID and LQR controllers, which are available on the Quanser website.

In the first two scenarios, we have considered two cases (Sections 4.1 and 4.2) for the computer-based numerical simulation and the last scenario is provided for experimental validation (Section 4.3). In the first scenario, the proposed simple learning-based controller is utilized to generate control actions for sinusoidal trajectories while in the second scenario, it is utilized for maintaining the system to track constant trajectories. In the numerical simulation scenarios, the total simulation time is 60 s. All experimental implementations are carried out on a platform with the following specifications: Windows 10 Enterprise; Processor: Intel(R) Core(TM) i7-9700 CPU @ 3.00 GHz, 3000 Mhz, 8 Core(s), 8 Logical Processor(s); RAM: 32.0 GB.

Table 1. System Parameters.

Symbol	Parameter	Value	Unit
J_p	Pitch inertia	0.0215	kg· m^2
J_y	Yaw inertia	0.037	kg· m^2
l_{cm}	Distance b/w center of mass and origin of B	0.002	m
m	Mass	1.075	kg
D_p	Pitch viscous friction coefficient	00071	$\frac{\text{N}}{\text{V}}$
D_y	Yaw viscous friction coefficient	0022	$\frac{\text{N}}{\text{V}}$
K_{pp}	Pitch torque thrust gain from pitch prop	0.0011	$\frac{\text{N·m}}{\text{V}}$
K_{py}	Pitch torque thrust gain from yaw prop	0.0007	$\frac{\text{N·m}}{\text{V}}$
K_{yp}	Yaw torque thrust gain from pitch prop	-0.0027	$\frac{\text{N·m}}{\text{V}}$
K_{yy}	Yaw torque thrust gain from yaw prop	0.0022	$\frac{\text{N·m}}{\text{V}}$

Table 2. Estimated System Parameters.

Symbol	Parameter	Value	Unit
$\hat{K}_{pp}$	Est. Pitch torque thrust gain from pitch prop	0.0008	$\frac{\text{N·m}}{\text{V}}$
$\hat{K}_{py}$	Est. Pitch torque thrust gain from yaw prop	0.00046	$\frac{\text{N·m}}{\text{V}}$
$\hat{K}_{yp}$	Est. Yaw torque thrust gain from pitch prop	-0.0014	$\frac{\text{N·m}}{\text{V}}$
$\hat{K}_{yy}$	Est. Yaw torque thrust gain from yaw prop	0.0028	$\frac{\text{N·m}}{\text{V}}$

The initial conditions for the simulations are selected as

$$(\theta_0, \psi_0) = (0, 0) \quad [deg]$$
$$(\dot{\theta}_0, \dot{\psi}_0) = (0, 0) \quad [deg/s]$$

The expressions for the desired closed-loop pitch and yaw error dynamics are given by

$$c_p(e, k^{\text{des}}) = \ddot{e}_p + k_{p_2}^{\text{des}} \dot{e}_p + k_{p_1}^{\text{des}} e_p \tag{25}$$
$$c_y(e, k^{\text{des}}) = \ddot{e}_y + k_{y_2}^{\text{des}} \dot{e}_y + k_{y_1}^{\text{des}} e_y \tag{26}$$

where (e_p, e_y) are the pitch and yaw errors, $(\dot{e}_p, \dot{e}_y)$ are the pitch rate and yaw rate errors, and $(\ddot{e}_p, \ddot{e}_y)$ are the pitch acceleration and yaw acceleration errors. The parameters $(k_{p_1}^{\text{des}}, k_{y_1}^{\text{des}})$ and $(k_{p_2}^{\text{des}}, k_{y_2}^{\text{des}})$ are the desired simple-learning gains for the pitch and yaw angles and their rates, respectively.

The following gains for the desired closed-loop error dynamics are used in both cases (Sections 4.1 and 4.2) for the simulation:

$$k_{p_1}^{\text{des}} = 4, \; k_{y_1}^{\text{des}} = 4$$
$$k_{p_2}^{\text{des}} = 4, \; k_{y_2}^{\text{des}} = 4$$

The initial controller gains and their learning rates are given by

$$k_{p_1}(0) = 5, \; k_{y_1}(0) = 5$$
$$k_{p_2}(0) = 3, \; k_{y_2}(0) = 3$$
$$\alpha_{p_1} = 1, \; \alpha_{y_1} = 1$$
$$\alpha_{p_2} = 1, \; \alpha_{y_2} = 1$$

In both simulation scenarios, external torques equal to $0.5\ N \cdot m$ are imposed on both pitch and yaw as external disturbances. The initial disturbances and disturbance learning rates are as follows

$$\hat{d}_p(0) = 0,\ \hat{d}_y(0) = 0$$
$$\alpha_{\hat{d}_p} = 1,\ \alpha_{\hat{d}_y} = 1$$

4.1. Case I: Tracking Sinusoidal Trajectories

In the first simulation, time-varying trajectory tracking control of the 2-DOF helicopter is investigated. The desired trajectory is given as the following:

$$\theta_d(t) = 10\cos t \quad [deg]$$
$$\psi_d(t) = 45\sin\frac{t}{4} \quad [deg]$$

Figure 2 shows the sinusoidal time-varying desired trajectories and the tracking outputs of the system where the proposed controller is in green (solid line), the LQR in magenta (dotted line), the PID in cyan (dashed-dotted line), and the desired trajectory in black (dashed line). The control gains (k_{p_1}, k_{p_2}) and (k_{y_1}, k_{y_2}), the estimated disturbances $(\hat{d}_p, \hat{d}_y)$, and the control input voltages (V_p, V_y) for Case I are shown in Figures 3–6.

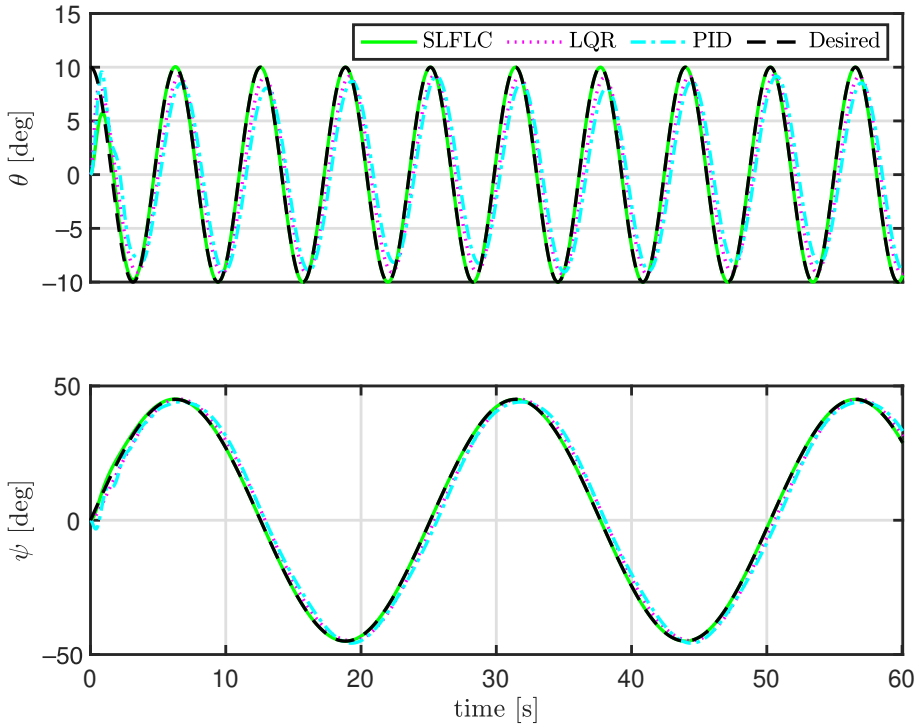

Figure 2. Trajectory tracking (Case I-simulation).

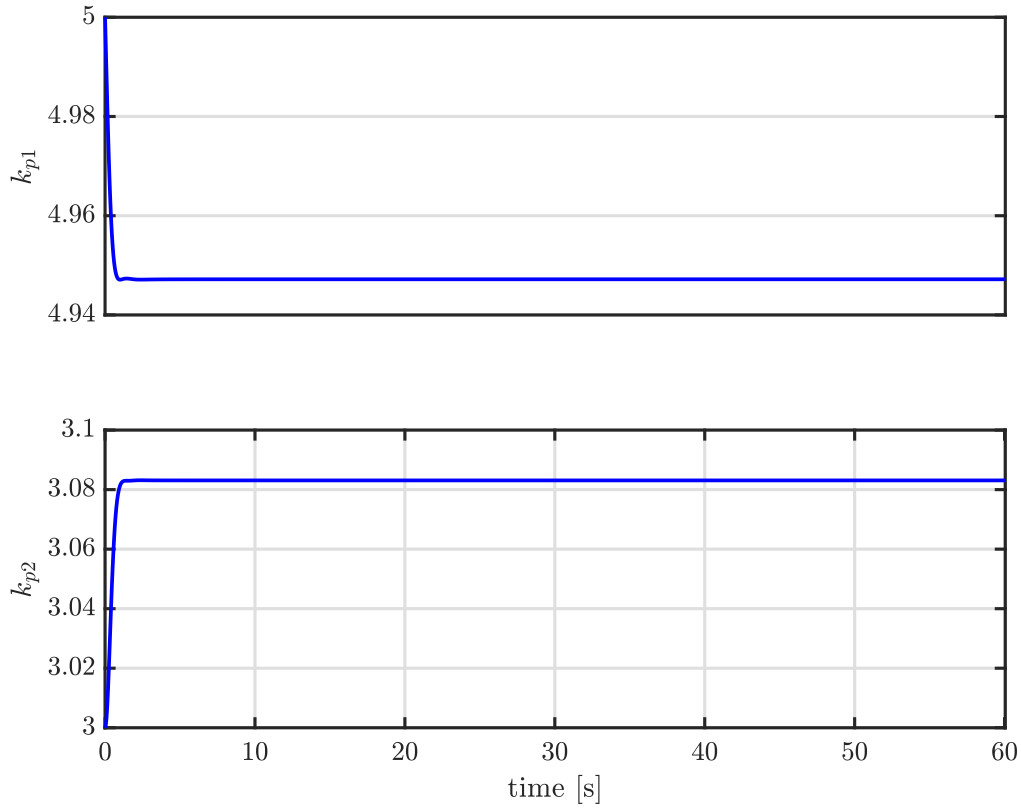

Figure 3. Control gains for pitch control (Case I-simulation).

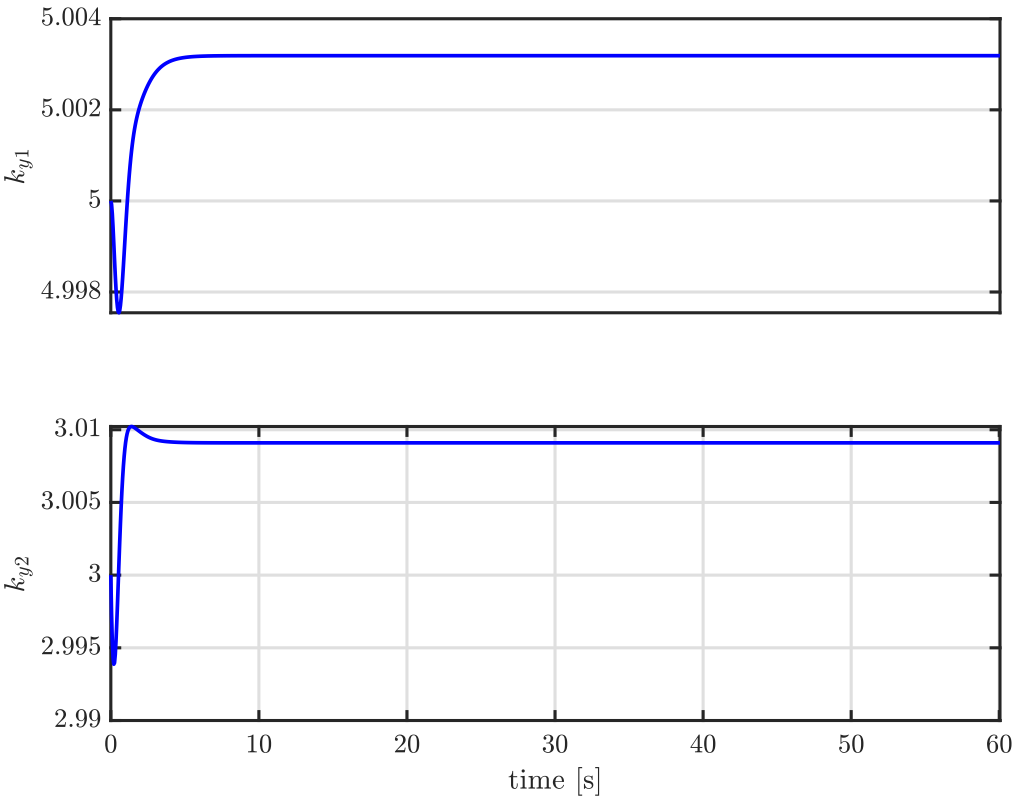

Figure 4. Control gains for yaw control (Case I-simulation).

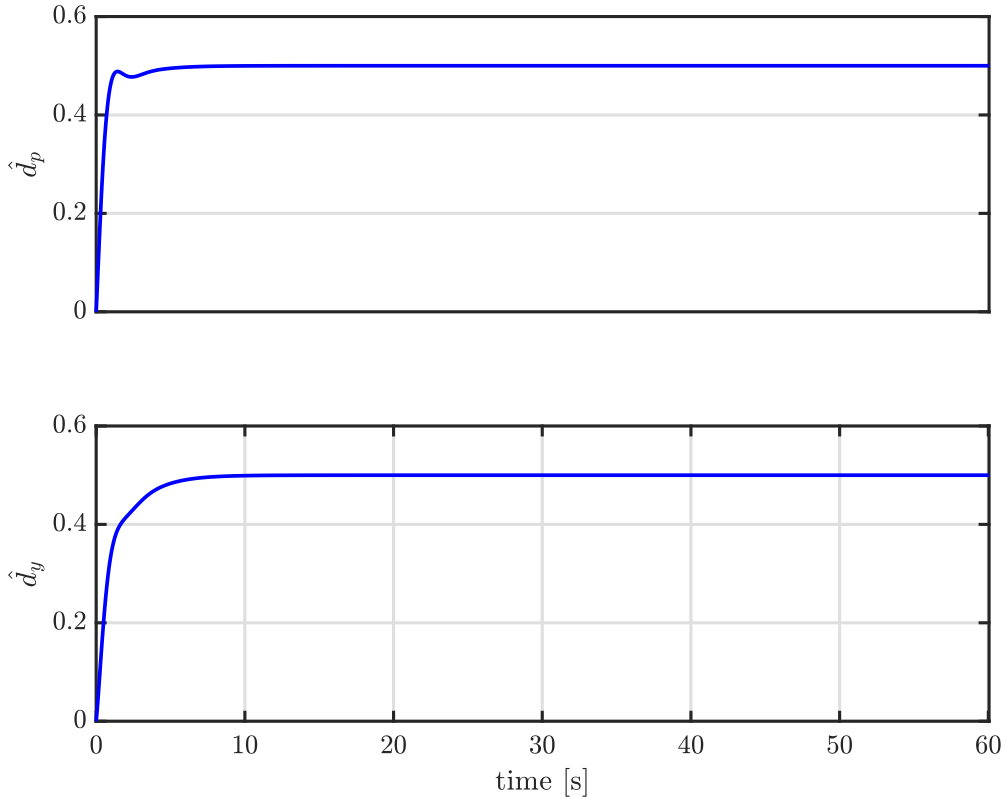

Figure 5. Estimated disturbances (Case I-simulation).

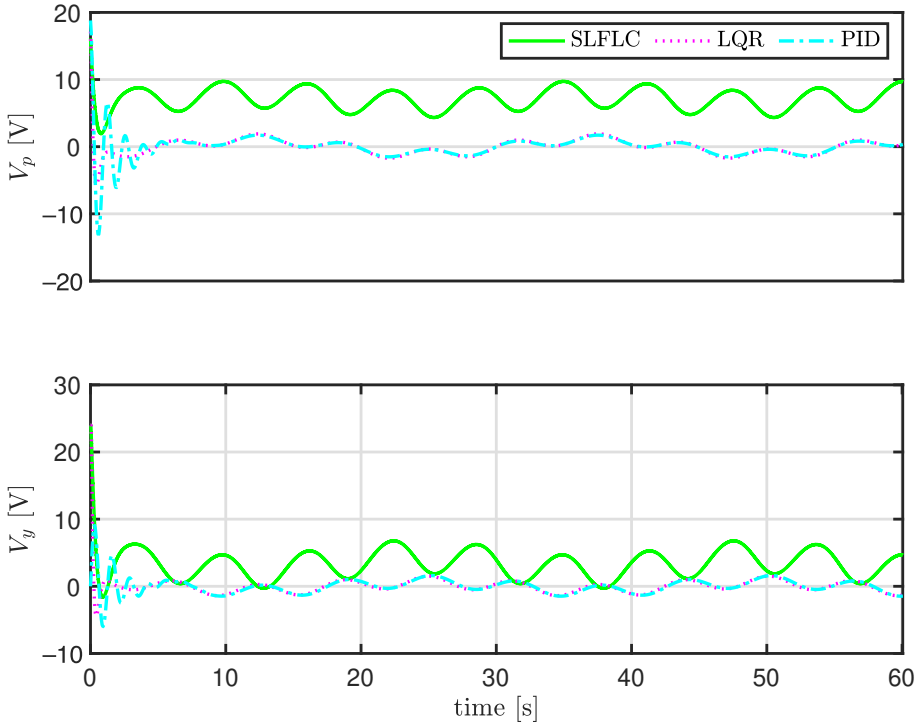

Figure 6. Input voltages (Case I-simulation).

By looking at Figure 2, we can observe that the pitch and yaw angles perfectly tracks the reference trajectory by using all the controllers; however, it is worth noting that the

performance of the proposed controller is superior compared to the other two controllers (LQR and PID) especially in tracking the pitch angle.

4.2. Case II: Tracking Constant Trajectories

In the second simulation, constant trajectory tracking control of the 2-DOF helicopter is investigated. The following set point is considered as the desired trajectory:

$$(\theta_d(t), \psi_d(t)) = (-10, 45) \quad [deg]$$

Figure 7 shows the constant desired trajectories and the tracking outputs of the system where the proposed controller is in green (solid line), the LQR in magenta (dotted line), the PID in cyan (dashed-dotted line), and the desired trajectory in black (dashed line). The control gains (k_{p_1}, k_{p_2}), and (k_{y_1}, k_{y_2}), the estimated disturbances $(\hat{d}_p, \hat{d}_y)$, and the control input voltages (V_p, V_y) for Case II are shown in Figures 8–11.

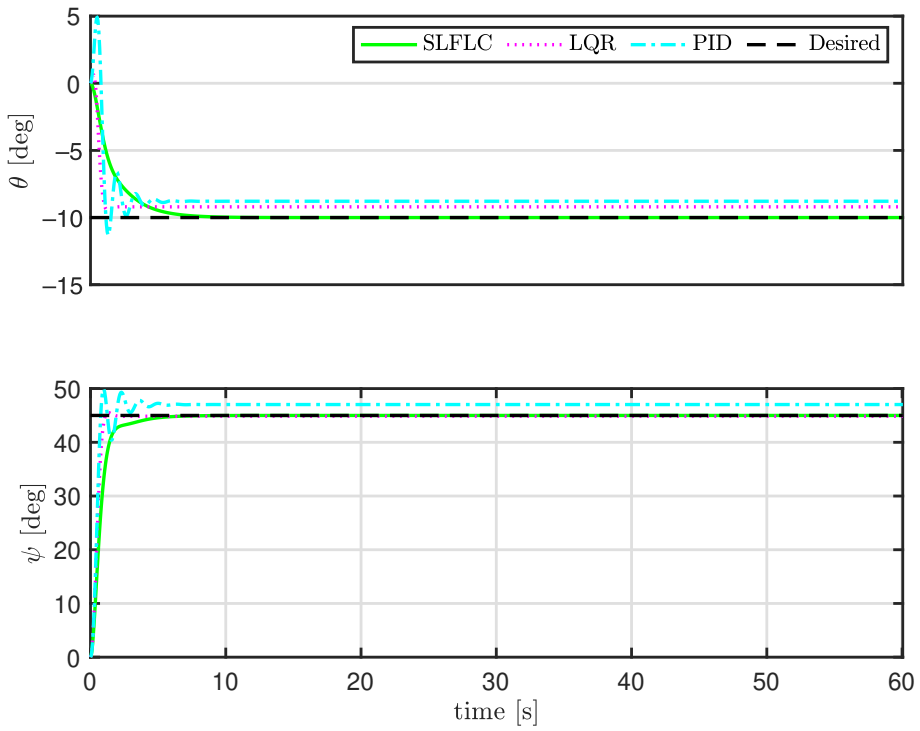

Figure 7. Trajectory tracking (Case II-simulation).

As seen in Figure 7, the pitch and yaw angles converge to the desired set point; however, the performance of the other two controllers (LQR and PID) especially in tracking the pitch angle is degraded. It is worth noting that the parameters of all the controllers remained the same as in the previous scenario (i.e., Section 4.1), which further validates the effectiveness of the proposed controller under varying conditions.

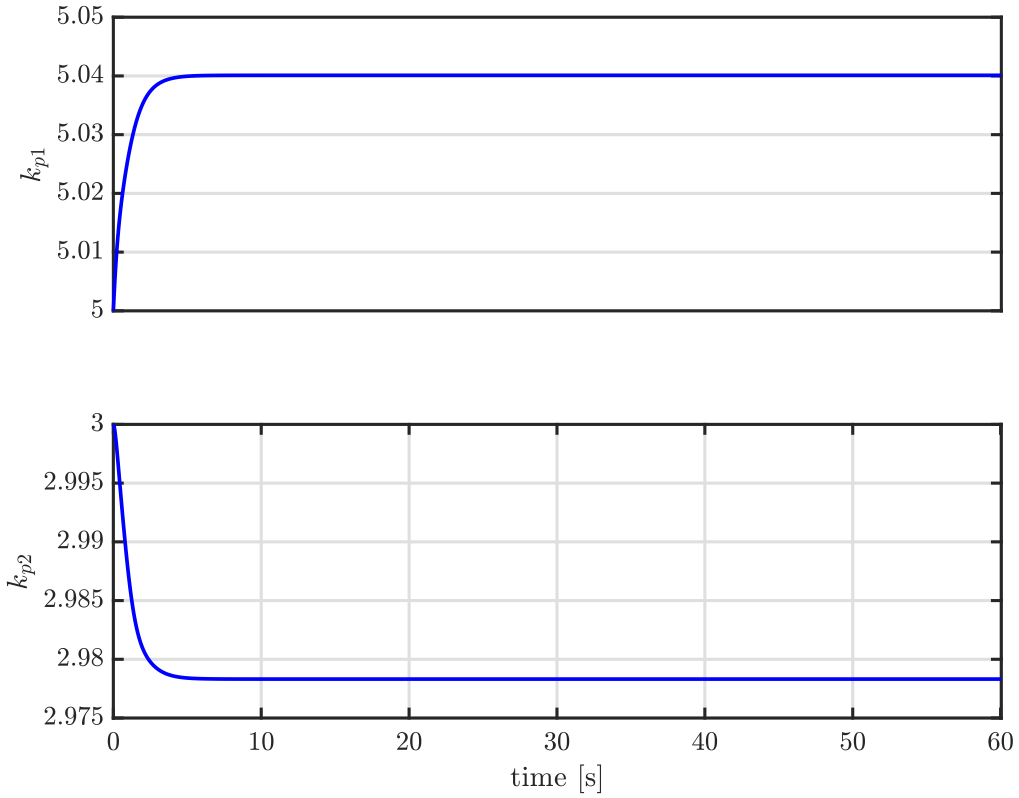

Figure 8. Control gains for pitch control (Case II-simulation).

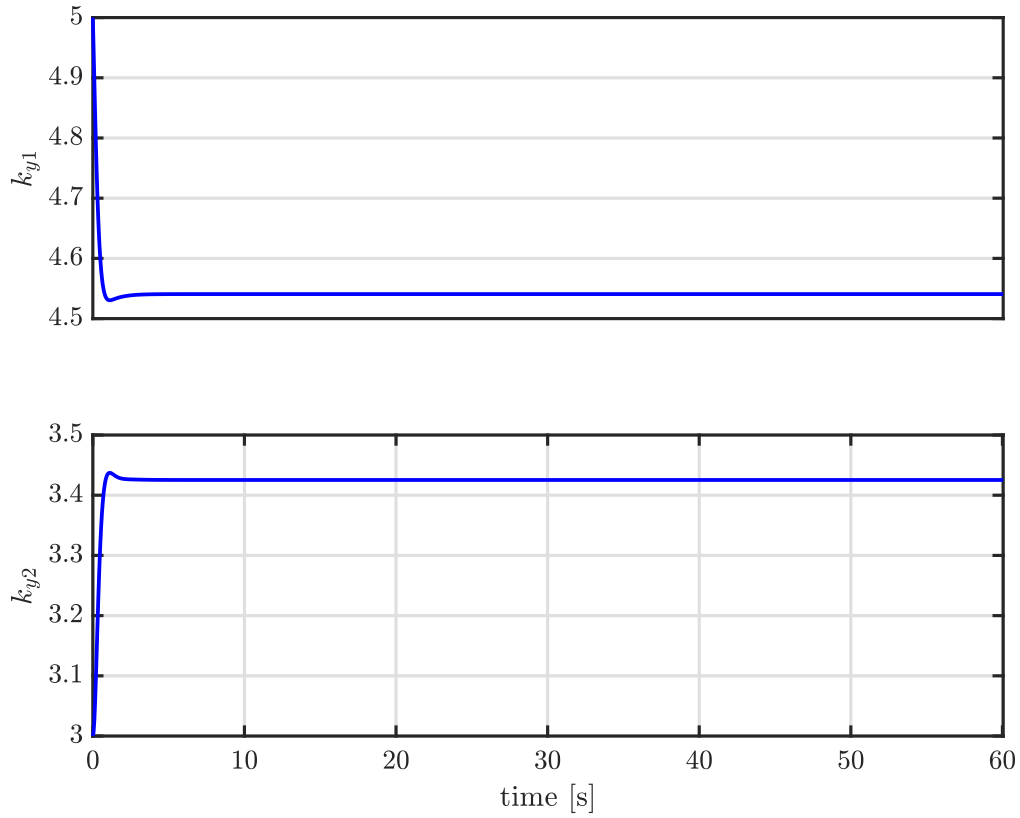

Figure 9. Control gains for yaw control (Case II-simulation).

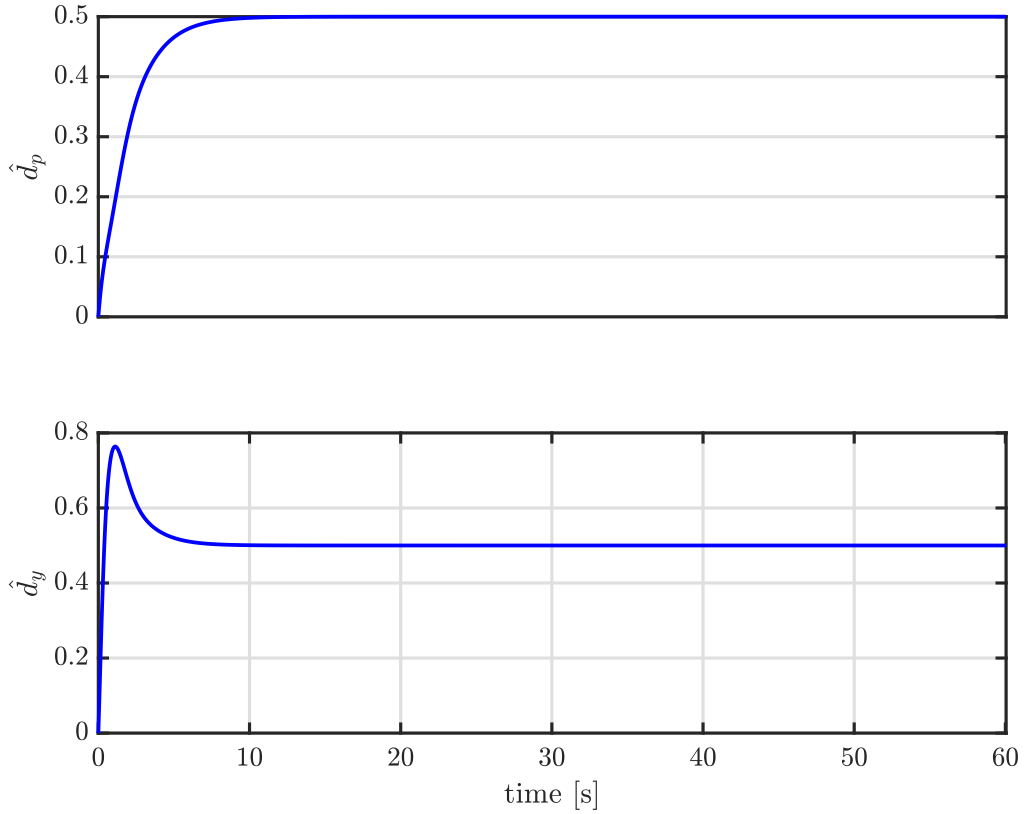

Figure 10. Estimated disturbances (Case II-simulation).

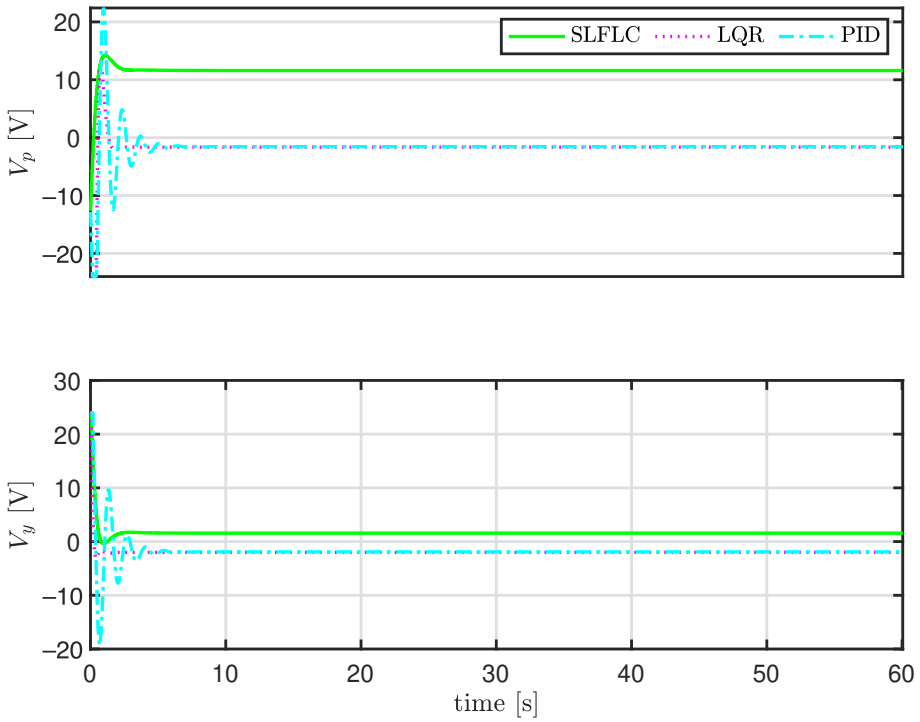

Figure 11. Input voltages (case II-simulation).

4.3. Case III: Experiment

We experimentally validated our proposed method on the Quanser 2-DOF AERO 2-DOF helicopter system testbed (see Figure 12). The desired trajectory is given as:

$$\theta_d(t) = 10 \sin t \quad [deg]$$
$$\psi_d(t) = 45 \sin \frac{t}{4} \quad [deg]$$

The following gains for the desired closed-loop error dynamics are used for experimental validation:

$$k_{p_1}^{\text{des}} = 550,\ k_{y_1}^{\text{des}} = 50$$
$$k_{p_2}^{\text{des}} = 50,\ k_{y_2}^{\text{des}} = 50$$

The initial controller gains and their learning rates are given by

$$k_{p_1}(0) = 8,\ k_{y_1}(0) = 8$$
$$k_{p_2}(0) = 8,\ k_{y_2}(0) = 8$$
$$\alpha_{p_1} = 1,\ \alpha_{y_1} = 1$$
$$\alpha_{p_2} = 1,\ \alpha_{y_2} = 1$$

The disturbance vector is initialized as

$$\hat{d}_p(0) = 0,\ \hat{d}_y(0) = 0$$

The disturbance learning rates are

$$\alpha_{\hat{d}_p} = 1,\ \alpha_{\hat{d}_y} = 1$$

Figure 13 shows the sinusoidal time-varying desired trajectories and the tracking outputs of the system where the proposed controller is in green (solid line), the LQR in magenta (dotted line), the PID in cyan (dashed-dotted line), and the desired trajectory in black (dashed line). The control gains (k_{p_1}, k_{p_2}), and (k_{y_1}, k_{y_2}), the estimated disturbances $(\hat{d}_p, \hat{d}_y)$, and the control input voltages (V_p, V_y) for Case III are shown in Figures 14–17.

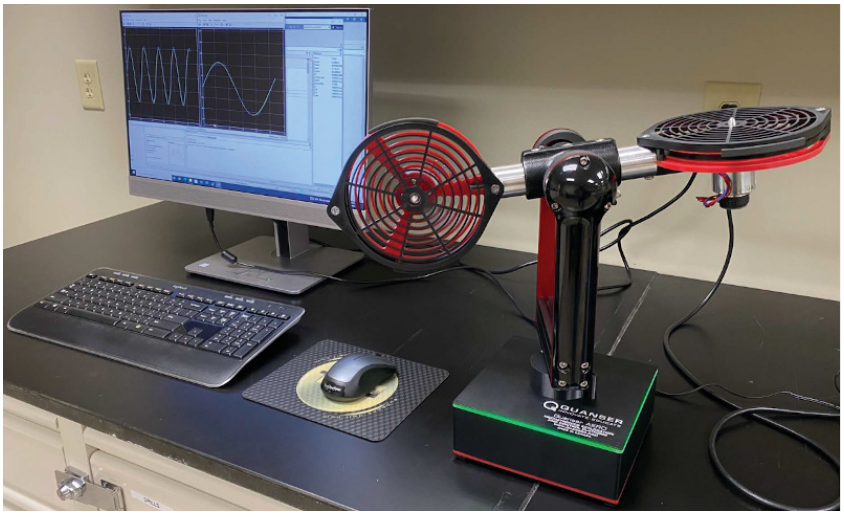

Figure 12. Quanser 2-DOF AERO 2-DOF helicopter system testbed.

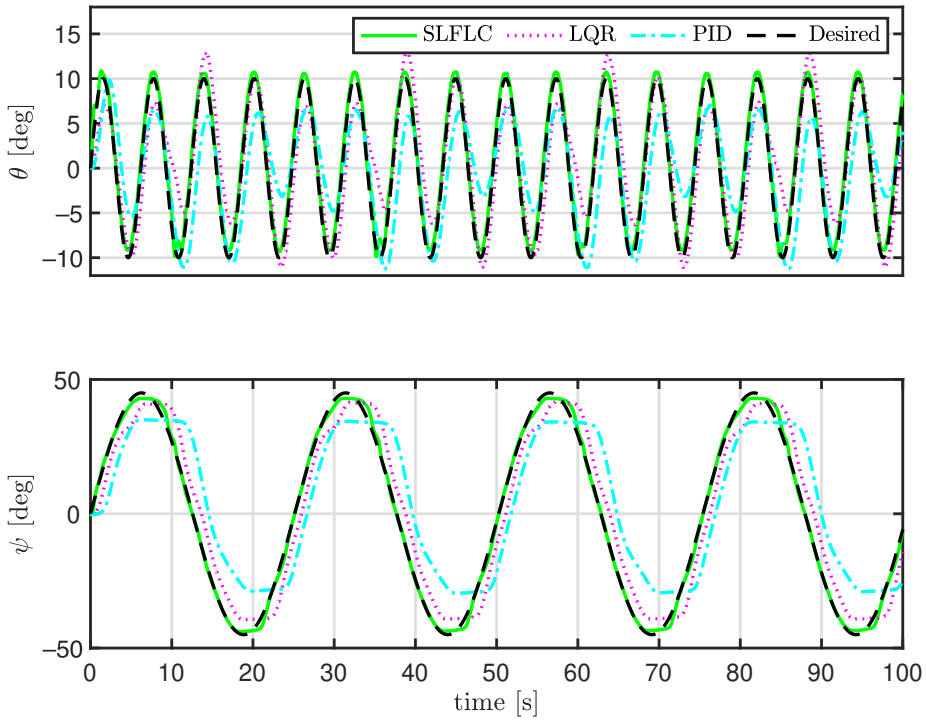

Figure 13. Trajectory tracking (Case III-experiment).

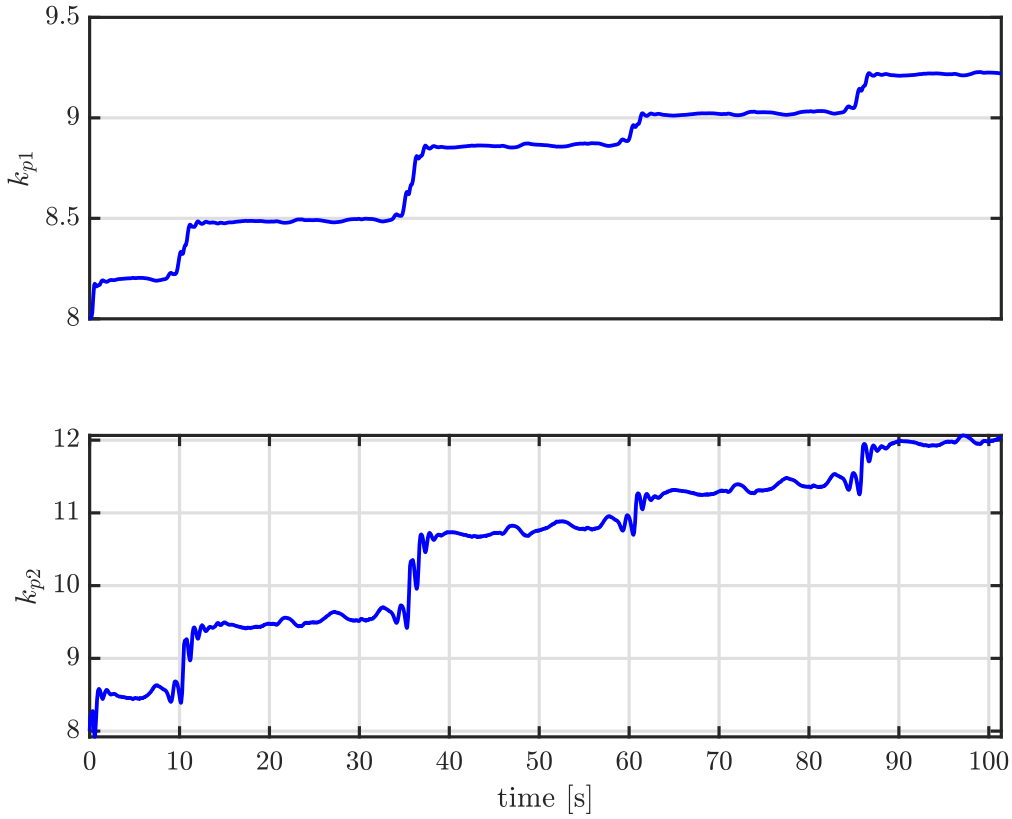

Figure 14. Control gains for pitch control (Case III-experiment).

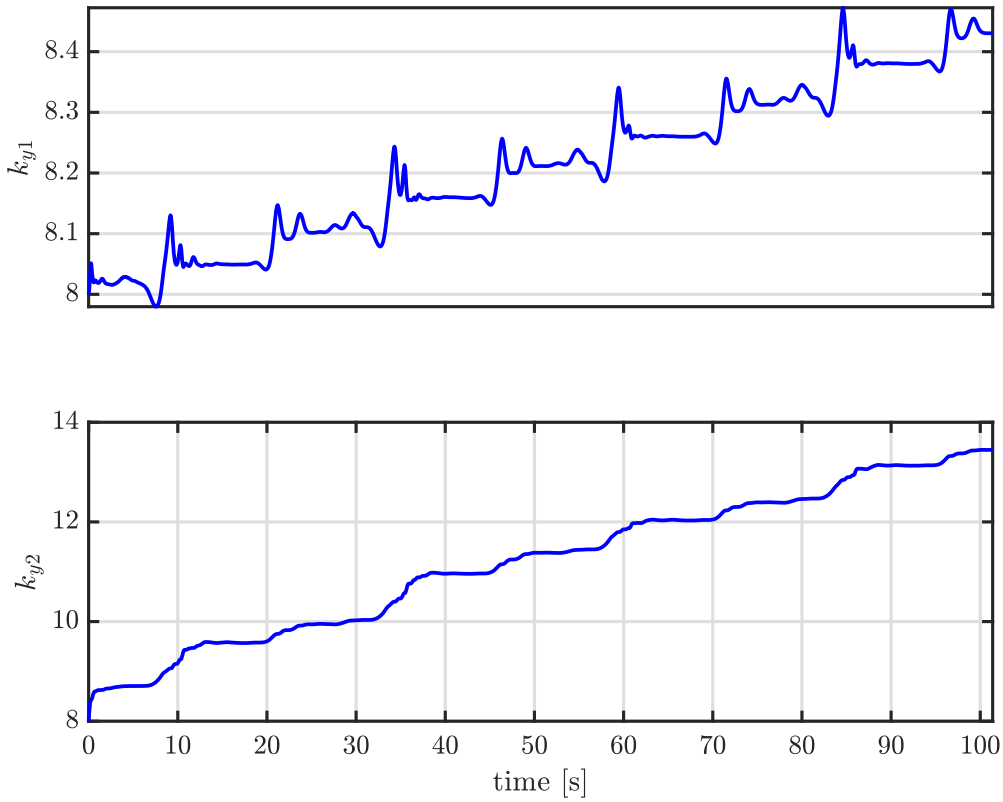

Figure 15. Control gains for yaw control (Case III-experiment).

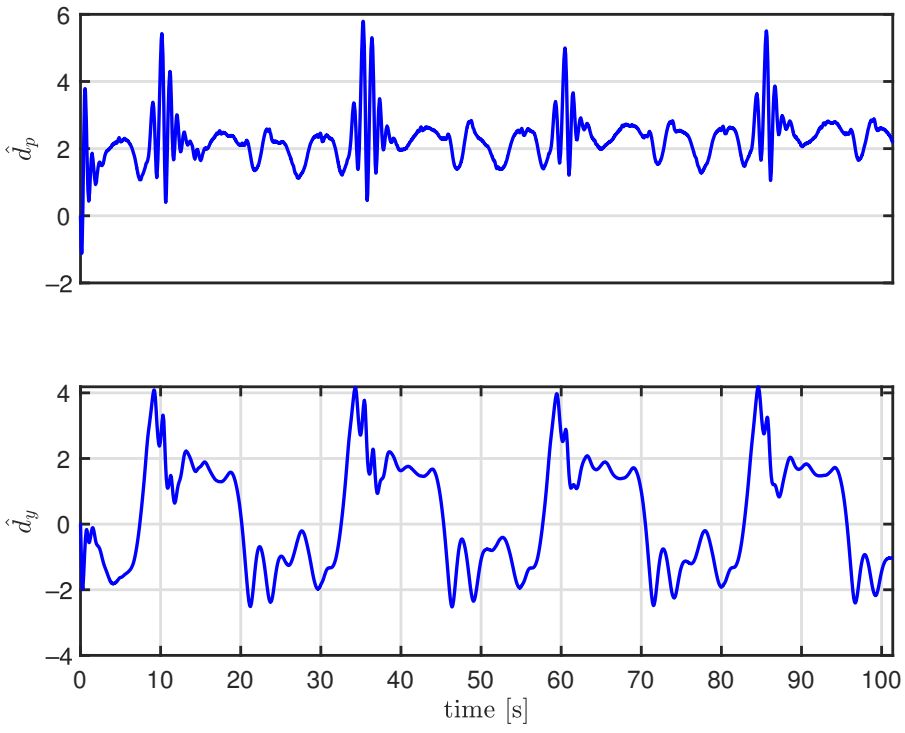

Figure 16. Estimated disturbances (Case III-experiment).

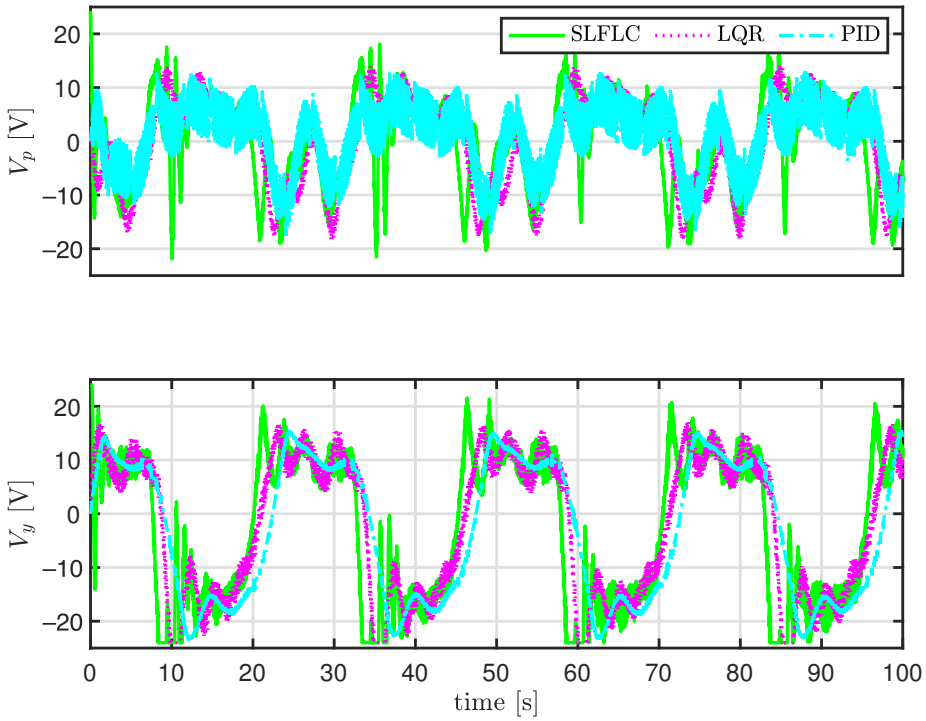

Figure 17. Input voltages (Case III-experiment).

As seen in Figure 13, the pitch and yaw angles track the desired trajectory perfectly; however, the performance of the other two controllers (LQR and PID) especially in tracking the pitch angle is degraded.

5. Conclusions

A trajectory tracking control strategy for a 2-DOF helicopter system testbed is presented in this paper. The proposed learning strategy compensates for model uncertainties and disturbances. This is performed by designing a gradient descent-based simple learning control strategy that minimizes the cost function defined by the error dynamics of the nonlinear system. The effectiveness of the attitude trajectory tracking control method is validated through both computer simulation and experimental results. Comparison with the well-known existing methods such as LQR and PID controllers further validate the satisfactory performance of the developed method.

Future work will consider extending our results by designing an approximator to estimate the system parameters in real-time, which will make the current architecture less dependent on the knowledge of the system.

Author Contributions: M.R. (Mahmut Reyhanoglu) performed the analysis and wrote the original draft. M.J. obtained the computational and experimental results, and contributed to the editing of the manuscript. M.R. (Muhammad Rehan) contributed to the simulation and writing. All authors have read and agreed to the published version of the manuscript.

Funding: This research received no external funding.

Data Availability Statement: Not applicable.

Acknowledgments: The first and second authors wish to acknowledge the support provided by Columbus State University, USA.

Conflicts of Interest: The authors declare no conflict of interest.

References

1. Valavanis, K.P.; Vachtsevanos, G.J. *Handbook of Unmanned Aerial Vehicles*; Springer: Berlin/Heidelberg, Germany, 2015; Volume 1.
2. Nourmohammadi, A.; Jafari, M.; Zander, T.O. A survey on unmanned aerial vehicle remote control using brain–computer interface. *IEEE Trans.-Hum.-Mach. Syst.* **2018**, *48*, 337–348.
3. Kayacan, E.; Khanesar, M.A.; Rubio-Hervas, J.; Reyhanoglu, M. Learning control of fixed-wing unmanned aerial vehicles using fuzzy neural networks. *Int. J. Aerosp. Eng.* **2017**, *10.1155/2017/5402809*.
4. Hervas, J.R.; Reyhanoglu, M.; Tang, H.; Kayacan, E. Nonlinear control of fixed-wing UAVs in presence of stochastic winds. *Commun. Nonlinear Sci. Numer. Simul.* **2016**, *33*, 57–69.
5. Nuthi, P.; Subbarao, K. Experimental verification of linear and adaptive control techniques for a two degrees-of-freedom helicopter. *J. Dyn. Syst. Meas. Control* **2015**, *137*, 064501.
6. Kumar, E.V.; Raaja, G.S.; Jerome, J. Adaptive PSO for optimal LQR tracking control of 2 DoF laboratory helicopter. *Appl. Soft Comput.* **2016**, *41*, 77–90.
7. Butt, S.S.; Sun, H.; Aschemann, H. Control design by extended linearisation techniques for a two degrees of freedom helicopter. *IFAC-Pap.* **2015**, *48*, 22–27.
8. Luo, B.; Wu, H.N.; Huang, T. Optimal output regulation for model-free Quanser helicopter with multistep Q-learning. *IEEE Trans. Ind. Electron.* **2017**, *65*, 4953–4961.
9. Lambert, P.; Reyhanoglu, M. Observer-based sliding mode control of a 2-DOF helicopter system. In Proceedings of the IECON 2018—44th Annual Conference of the IEEE Industrial Electronics Society, Washington, DC, USA, 21–23 October 2018; pp. 2596–2600.
10. Steinbusch, A.; Reyhanoglu, M. Robust nonlinear tracking control of a 2-dof helicopter system. In Proceedings of the 2019 12th Asian Control Conference (ASCC), Kitakyushu, Japan, 9–12 June 2019; pp. 1649–1654.
11. Marconi, L.; Naldi, R. Robust full degree-of-freedom tracking control of a helicopter. *Automatica* **2007**, *43*, 1909–1920.
12. Kadmiry, B.; Driankov, D. A fuzzy gain-scheduler for the attitude control of an unmanned helicopter. *IEEE Trans. Fuzzy Syst.* **2004**, *12*, 502–515.
13. Vilchis, J.A.; Brogliato, B.; Dzul, A.; Lozano, R. Nonlinear modelling and control of helicopters. *Automatica* **2003**, *39*, 1583–1596.
14. Raptis, I.A.; Valavanis, K.P.; Moreno, W.A. A novel nonlinear backstepping controller design for helicopters using the rotation matrix. *IEEE Trans. Control Syst. Technol.* **2010**, *19*, 465–473.
15. Bogdanov, A.; Wan, E. State-dependent Riccati equation control for small autonomous helicopters. *J. Guid. Control Dyn.* **2007**, *30*, 47–60.
16. Labdai, S.; Chrifi-Alaoui, L.; Drid, S.; Delahoche, L.; Bussy, P. Real-time implementation of an optimized fractional sliding mode controller on the quanser-aero helicopter. In Proceedings of the 2020 International Conference on Control, Automation and Diagnosis (ICCAD), Paris, France, 7–9 October 2020; pp. 1–6.
17. Fandel, A.; Birge, A.; Miah, S. Development of reinforcement learning algorithm for 2-dof helicopter model. In Proceedings of the 2018 IEEE 27th International Symposium on Industrial Electronics (ISIE), Cairns, QLD, Australia, 13–15 June 2018; pp. 553–558.
18. Abdelmaksoud, S.I.; Mailah, M.; Abdallah, A.M. Practical real-time implementation of a disturbance rejection control scheme for a twin-rotor helicopter system using intelligent active force control. *IEEE Access* **2020**, *9*, 4886–4901.
19. Kim, S.K.; Ahn, C.K. Performance-Boosting Attitude Control for 2-DOF Helicopter Applications via Surface Stabilization Approach. *IEEE Trans. Ind. Electron.* **2021**, *69*, 7234–7243.
20. Mehndiratta, M.; Kayacan, E.; Reyhanoglu, M.; Kayacan, E. Robust tracking control of aerial robots via a simple learning strategy-based feedback linearization. *IEEE Access* **2019**, *8*, 1653–1669.
21. Jafari, M.; Xu, H. Intelligent control for unmanned aerial systems with system uncertainties and disturbances using artificial neural network. *Drones* **2018**, *2*, 30.
22. Steinbusch, A.; Reyhanoglu, M. Robust Nonlinear Output Feedback Control of a 6-DOF Quadrotor UAV. In Proceedings of the 2019 12th Asian Control Conference (ASCC), Kitakyushu, Japan, 9–12 June 2019; pp. 1655–1660.
23. Jafari, M.; Shahri, A.M.; Shouraki, S.B. Attitude control of a quadrotor using brain emotional learning based intelligent controller. In Proceedings of the 2013 13th Iranian Conference on Fuzzy Systems (IFSC), Qazvin, Iran, 27–29 August 2013; pp. 1–5.
24. Lambert, P.; Reyhanoglu, M. Observer-based sliding mode control of a 6-DOF quadrotor UAV. In Proceedings of the IECON 2018—44th Annual Conference of the IEEE Industrial Electronics Society, Washington, DC, USA, 21–23 October 2018; pp. 2379–2384.
25. Hoffman, D.; Rehan, M.; MacKunis, W.; Reyhanoglu, M. Quaternion-based robust trajectory tracking control of a quadrotor hover system. *Int. J. Control Autom. Syst.* **2018**, *16*, 2575–2584.
26. Jafari, M.; Xu, H.; Garcia Carrillo, L.R. A neurobiologically-inspired intelligent trajectory tracking control for unmanned aircraft systems with uncertain system dynamics and disturbance. *Trans. Inst. Meas. Control* **2019**, *41*, 417–432.
27. Ligthart, J.A.; Poksawat, P.; Wang, L.; Nijmeijer, H. Experimentally validated model predictive controller for a hexacopter. *IFAC-Pap.* **2017**, *50*, 4076–4081.
28. Schlanbusch, S.; Zhou, J. Adaptive backstepping control of a 2-dof helicopter. In Proceedings of the 2019 7th International Conference on Control, Mechatronics and Automation (ICCMA), Delft, The Netherlands, 6–8 November 2019; pp. 210–215.
29. Roy, S.; Baldi, S.; Fridman, L.M. On adaptive sliding mode control without a priori bounded uncertainty. *Automatica* **2020**, *111*, 108650.

30. Sankaranarayanan, V.N.; Roy, S.; Baldi, S. Aerial transportation of unknown payloads: Adaptive path tracking for quadrotors. In Proceedings of the 2020 IEEE/RSJ International Conference on Intelligent Robots and Systems (IROS), Las Vegas, NV, USA, 24 October 2020–24 January 2021; pp. 7710–7715.
31. Langson, W.; Alleyne, A. A stability result with application to nonlinear regulation: Theory and experiments. In Proceedings of the 1999 American Control Conference (Cat. No. 99CH36251), San Diego, CA, USA, 2–4 June 1999; Volume 5, pp. 3051–3056.